Journal of
Mechanical
Science and
Technology

Journal of Mechanical Science and Technology 21 (2007) 1367~1375

Separation Control Mechanism of Airfoil Using Synthetic Jet

Sang Hoon Kim, Wooram Hong, Chongam Kim*

Department of Mechanical and Aerospace Engineering, Seoul National University, Seoul 151-742, Korea

(Manuscript Received December 15, 2006; Revised March 20, 2007; Accepted May 2, 2007)

Abstract

Numerical simulation of separation control using a synthetic jet was performed on NACA23012 airfoil. The computed results showed that stall characteristics and control surface performance could be improved substantially by resizing the separation vortices. It was observed that actual flow control mechanism was fundamentally different depending on the range of synthetic jet frequency. For low frequency range, small vortices due to synthetic jet penetrated to the large leading edge separation vortex flow, and as a result, the size of the leading edge separation vortex remarkably decreased. For high frequency range, however, the small vortex did not grow enough to penetrate into the large separation vortex, but the synthetic jet changed airfoil circulation directly. The synthetic jet conditions for effective lift increase are as follows: the non-dimensional frequency of the synthetic jet is 1; the location of the synthetic jet slot is the same as the separation point; and the jet velocity is large enough to perturb the separated flow. By exploiting these conditions, it was observed that the combination of the synthetic jet with a simple high lift device could be as good as a conventional fowler flap system.

Keywords: Flow control; Separation control; Synthetic jet

1. Introduction

Since the flight of the Wright brothers, many researchers and engineers have attempted to increase lift and reduce drag, and these efforts have led to an efficient design of modern aircraft. Nowadays, aircrafts are developed for various missions of flight. The common demand of aircraft design is to improve global aircraft performance to satisfy various mission requirements. From this point of view, it is clear that the lift-to-drag ratio is the key aerodynamic factor. The aircraft providing a higher-lift may need a quicker and shorter take-off and landing distance. However, the existing high-lift generation systems do not satisfy the strict design requirement of a higher-efficiency and higher-performance aircraft system, so, as always, more efficient flow control strategy needs to be investigated.

Naturally, there have been continual research in the field of flow control and especially, on the flow control methods using a MEMS system since the 1990's by Ho et al. (1998) and Gad-el-Hak (2002). Basic flow control (ex: the delay of flow separation, transition control and so on) and precise attitude control, both of which profoundly affect the maneuverability of aircrafts, missiles and so on, are being actively studied. Among the flow control devices, the synthetic jet has become one of the actively studied subjects, because it has a potential to be implemented to an aircraft flow control system.

A schematic of a synthetic jet is shown in Fig. 1. A jet is generated by an oscillatory membrane within a cavity. Then, the surrounding fluid enters and exits the cavity through a slot. At the blowing phase, the membrane moves upward to eject fluid from the cavity. At the suction phase, the membrane move away from the slot exit to suck in fluid into the cavity.

*Corresponding author. Tel.: +82 2 880 1915, Fax.: +82 2 887 2662
E-mail address: chongam@snu.ac.kr

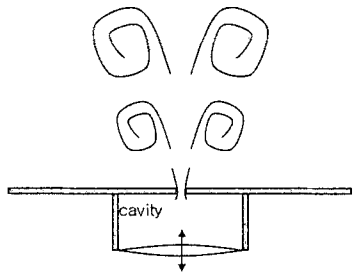

Fig. 1. Schematic of synthetic jet.

As a result, a vortex ring is formed between the discharged fluid and the surrounding fluid, and it is moved far away.

There have been numerous researches on the flow control using an oscillatory jet. Separation delay by acoustic excitation of an airfoil was investigated by F. Collins and J. Zelenevitz (1975) and followed by many others. Especially, an encouraging work was performed by I. Wygnanski and A. Seifert et al. (1993). They experimentally demonstrated the delay of airfoil stall by using an oscillatory blowing jet. It was found that the oscillatory blowing jet could delay separation much more efficiently than steady blowing, which had been traditionally used for this purpose. In the Defense Advanced Research Projects Agency (DARPA) Micro Adaptive Flow Control (MAFC) program, a full-scale flight test of the XV-15 experimental airplane was conducted by Nagib et al. (2003). The test results confirmed that the synthetic jet could provide 14% reduction in download forces during hovering by controlling local separated flow around the wing.

A. Glezer and M. Amitay et al. (2001a; 2001b) used a synthetic jet, positioned near the leading edge of a thick airfoil, to reattach the separated flow on the upper surface of the airfoil at stall and confirmed the reattachment of the separated flow and the movement of the separation point. In addition, D. Smith and A. Glezer et al. (2002) investigated controlled interactions of adjacent synthetic jets.

L. Kral et al. (1997) numerically simulated a synthetic jet actuator and obtained the results that were in good agreement with the experimental data of D. Smith and A. Glezer et al. They used an INS2D solver based on the Reynolds Averaged Navier-Stokes (RANS) approach. L. Kral et al. (1998) also carried out several numerical investigations on post-stall flow control. These results showed the benefits of the RANS-based numerical approach in the analysis of a synthetic jet flow.

In addition, the formation and evolution of a 3-D synthetic jet was studied in detail by using Direct Numerical Simulation (DNS) by R. Mittal et al. (2004). They also investigated the effect of the length-to- width ratio of a synthetic jet slot and the flow physics in the cavity of a synthetic jet actuator. Moreover, they observed the difference in the velocity distribution between the case with and the case without cavity.

However, the numerous studies about flow control using a synthetic jet mainly focused on low Reynolds number flows because the flow instability mechanism by turbulent transition was the main research interest and experimental studies on high Reynolds number flows were relatively difficult. The analysis of flow control characteristics at high Reynolds number, however, is very important because the results can provide valuable information on the feasibility of various flow control methods for aircraft application. Recently, active flow control strategy to increase lift was demonstrated at high Reynolds numbers, corresponding to a jet airplane at take-off conditions, by A. Seifert et al. (1999).

In the present paper, numerical simulations to understand the aerodynamic mechanism of separation control using synthetic jet on NACA23012 airfoil were performed. Flow control with a synthetic jet was carried out on NACA23012 with a 20% chord flap, and the flow characteristics of separation control on the leading edge and plain flap were studied. In addition, the combination of the synthetic jet with a simple high lift device on the effective flow control conditions was investigated.

2. Numerical methods

2.1 Governing equations

In this study, the two-dimensional unsteady incompressible Navier-Stokes equations were used to simulate unsteady separated flows. The incompressible governing equations are given by the continuity equation,

$$\nabla \cdot \bar{\mathbf{u}} = 0 \tag{1}$$

and momentum equations,

$$\rho \frac{\partial \bar{\mathbf{u}}}{\partial t} + \rho \bar{\mathbf{u}} \cdot \nabla \bar{\mathbf{u}} = -\nabla \bar{p} + (\mu + \mu_t) \nabla^2 \bar{\mathbf{u}} \tag{2}$$

for the conservation of mass and momentum, where the over-bar indicates a Reynolds-averaged quantity. The governing equations were then solved time-accurately by using the method of pseudo-compressibility [proposed by Chorin (1968)]. By using the MUSCL approach, the upwind differencing scheme based on flux-difference splitting was used to calculate the convective terms at third-order spatial accuracy. Viscous fluxes were then centrally differenced by using second-order spatial accuracy, and flow variables were updated by the LU-SGS time integration scheme of Yoon et al. (1991).

Turbulence model used in the present computation was the Menter's shear stress transport two-equation model. Bardina et al. (1997) reported that this turbulence model can provide excellent prediction of flows with separation. All computations were performed with a finite volume based in-house code, which has been extensively tested by Kim et al. (2000). In all calculations presented here, the boundary layer was assumed to be fully turbulent with the Reynolds number of 2.19×10^6.

2.2 Boundary condition of synthetic jet

Suction/blowing type boundary condition proposed by L. Kral et al. (1997) was adopted to model a synthetic jet actuator. Perturbation to the flow-field is introduced in terms of the velocity at the surface as

$$\bar{u}_n(\xi=0,\eta,t)=A_{jet}f(\eta)\sin(\omega t), \tag{3}$$

where ξ denotes the stream-wise direction, η denotes the cross-stream direction, and $\bar{u}_n$ is the stream-wise component of velocity. Spatial variations over the orifice is chosen as a top hat distribution as

$$f(\eta)=1 \tag{4}$$

L. Kral et al. (1997) proposed the top hat distribution because this distribution matched well with the experiment data. Pressure boundary condition at the solid surface is obtained by the momentum equation, which ignores viscous effects. The time harmonic velocity perturbation is considered and then boundary condition becomes

$$\frac{\partial\bar{p}}{\partial\xi}=-\rho\frac{\partial\bar{u}_n}{\partial t} \tag{5}$$

3. Results

Simulations in the present study were carried out using the following conditions: freestream velocity of U_∞ = 35.9 m/s and a chord Reynolds number of Re = 2.19×10^6 for various jet velocities and frequencies. The chord length of the airfoil was 914.4 mm (3 ft), and the width of the two-dimensional slot was 1.0 mm (about 0.11% chord). The NACA23012 airfoil with a 20% chord plain flap was used in the present study and is shown in Fig. 2.

3.1 NACA23012 baseline case

First, the basic test case without a synthetic jet was considered. The results of the uncontrolled NACA-23012 airfoil are shown in Fig. 3 and compared with

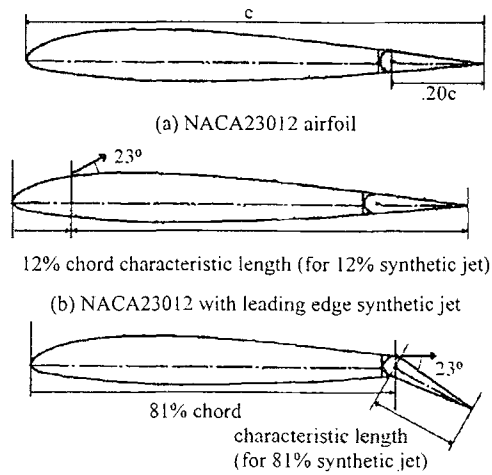

Fig. 2. Geometry of NACA23012 with a 20% plain flap.

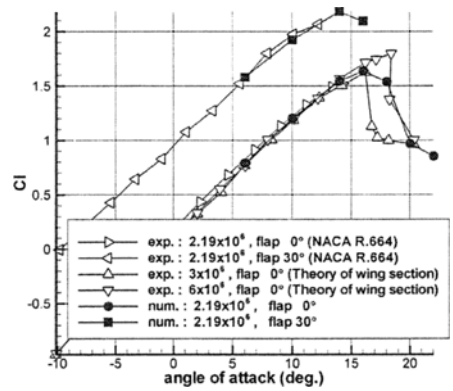

Fig. 3. Lift coefficient curves of NACA23012 (non-controlled case).

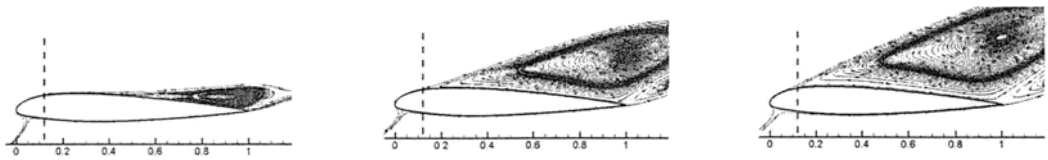

(1) AOA-18° (2) AOA-20° (3) AOA-22°

(a) Leading edge separation without flap deflection.

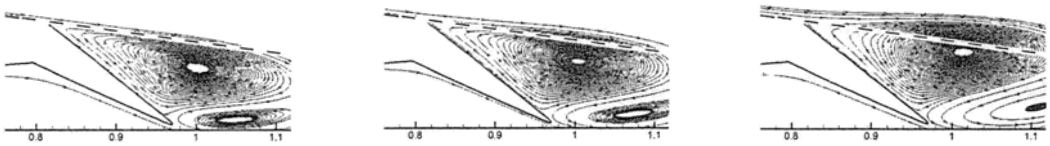

(1) AOA-6° (2) AOA-10° (3) AOA-14°

(b) Plain flap separation with 30° deflected flap.

Fig. 4. Phase-averaged streamlines of non-controlled case.

experimental data of Wenzinger et al. (1939) and Abbott et al. (1959). Figure 3 depicts the lift coefficient versus the angle of attack and the experimental data. The results agree fairly well with the experimental data except at the position of stall. However, the general behavior in the post-stall region is captured accurately enough to understand the main characteristics of flow physics. Prediction of precise stall characteristics with or without turbulence models is still an extremely challenging task, but current numerical models based on 2-D unsteady RANS equations provide fairly accurate information on global flow physics related to the separated or attached flows.

Figure 4 shows the streamlines of the uncontrolled case. In Fig. 4(a), for the uncontrolled case with an angle of attack of 18° with no-flap deflection, the flow was separated at the trailing edge region of the suction surface. At an angle of attack of 20°, the flow was separated at about the 12% chord from the leading edge and at the angle of attack was 22°, the separation point was moved a little bit forward. At an angle of attack of 20° and 22°, a large separation region occupied the flow field on the suction surface without reattachment. Thus, the proper location of the synthetic jet would be at the 12% chord from the leading edge in the controlled case.

In Fig. 4(b), for the case of a plain flap, the flow on the suction surface was separated for all angles of attack considered. The results show that the separation tendency was more intensified with increasing angle of attack. In these cases, the angle between the separation streamline and the plain flap increased with the angle of attack from 6° to 14°, but the position of separation did not move forward. The flow separated at the leading edge of the plain flap. Again, the separation region occupied the whole flow field on the suction surface of the plain flap without reattachment.

3.2 NACA23012 controlled case

Computations for a controlled NACA23012 airfoil were performed with a leading edge synthetic jet. Also, a NACA23012 airfoil with a 30° deflected plain flap was used for simulations of a plain flap synthetic jet. Based on the previous computation, a leading edge synthetic jet was located on the suction surface at the 12% chord from the leading edge. These are described in Fig. 2(b). The inclined angle of the synthetic jet was 23° from the local airfoil surface and it was fixed for all cases. According to the authors' preliminary study, the effect of a tangential synthetic jet on separation control was larger than that of a normal-direction synthetic jet.

The case of a plain flap synthetic jet is shown in Fig. 2(c): a NACA23012 airfoil with a 20% chord plain flap deflected at 30°. Again, based on the previous computation, a jet was located on the suction surface at the 81% chord from the leading edge. Also, the inclined angle of the jet was 23° from the surface. In order to understand the overall flow characteristics of separation control using a synthetic jet, numerical simulation was performed by changing the major control parameters of the synthetic jet: jet peak velocity from 1 to 3 times of freestream value and a non-dimensional jet frequency ($F+$) of 0.5 ~ 5. The characteristic length used in the calculation of the non-

dimensional frequency is the distance between the trailing edge and the jet slot, as described in Fig. 2. The jet momentum coefficient (C_μ) is defined as the ratio of the momentum provided by the synthetic jet to the freestream momentum. From the definition of the non-dimensional frequency, it can be seen that the geometric distance influenced by the synthetic jet momentum is equal to airfoil chord length when the non-dimensional frequency is 1. Similarly, the geometric distance is reduced to half-chord length when the non-dimensional frequency is 2.

For the purpose of simplicity, 'F1' denotes a non-dimensional frequency of 1; 'F2' is a non-dimensional frequency of 2; and 'F5' is a non-dimensional frequency of 5. Similarly, 'V1' indicates the amplitude of the synthetic jet peak velocity is equal to the freesteam velocity; 'V2' means it is double the value of the freesteam velocity; and 'V3' represents the synthetic jet peak velocity is the triple of the freestream velocity. Also, 'LE12p' implies the location of a synthetic jet slot is the 12% chord from the leading edge.

3.2.1 Leading edge separation control

Computations were performed for a leading edge synthetic jet. Figure 5(a) shows a comparison between baseline and controlled results. As shown in the figures, the synthetic jet yields the largest effect on the improvement of the lift coefficient when the non-dimensional frequency is 1. Also, the lift coefficient increases with the amplitude of the synthetic jet velocity at the same non-dimensional frequency, as expected. These results show that the leading edge synthetic jet did improve stall characteristics and increased the maximum lift coefficient. At an angle of attack of 22°, the maximum lift was obtained at a non-dimensional frequency of 1, as mentioned. The improvement in lift, which was almost 110% higher compared to the uncontrolled case, is shown in Fig. 5. In Fig. 4(a) of the uncontrolled case, at an angle of attack of 22°, the separation point was very near the synthetic jet slot. Therefore, the conditions of the maximum lift enhancement can be as follows: the non-dimensional frequency is 1; the location of the synthetic jet slot is equal to the separation point; and the jet velocity is large enough to perturb the surrounding separated flow.

3.2.2 Plain flap separation control

A NACA23012 airfoil with a 30° deflected plain

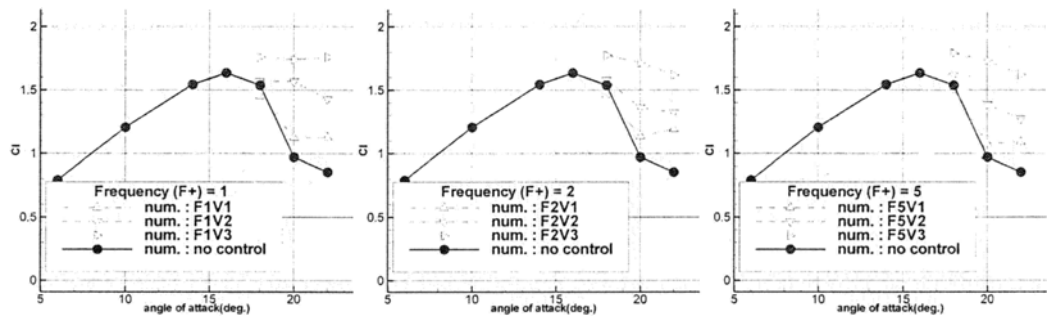

(a) On 0.12c

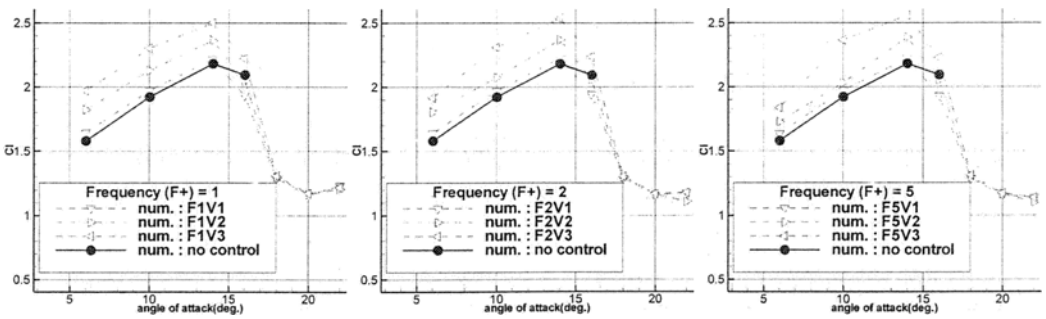

(b) On 0.81c with a deflected plain flap

Fig. 5. Lift coefficient curves.

flap was simulated. As shown in Fig. 5(b), the lift coefficient before stall angle greatly increased when the non-dimensional frequency was 1. Also, as the amplitude of the synthetic jet velocity increased, the lift coefficient increased at the same non-dimensional frequency. However, after an angle of attack of 16° at which the leading edge stall occurred, a similar tendency was not observed. On the contrary, the effect of the synthetic jet was not noticeable because the synthetic jet was located within the region of flow separation.

At an angle of attack of 6°, the lift coefficient increased in proportion to the amplitude of the synthetic jet velocity at the same non-dimensional frequency [Fig. 5(b)]. The maximum lift increase was obtained at a non-dimensional frequency of 1, which were the same result to the case of the leading edge synthetic jet. However, at an angle of attack of 10° and 14°, the maximum lift increase was obtained at the non-dimensional frequency of 5 in the case of 'V3' ($C\mu$ = 0.0177). This may be explained by the fact that the high frequency synthetic jet (F5) could control the local flow to attach firmly and to make a more stable flow structure. These results indicate that a high frequency jet can improve the control surface performance better than a low frequency jet. In the case of high frequency jet, the attachment effect of the separated flow was more prominent, and as a result, it stabilizes the local flow structure.

Therefore, there are differences between these results and the results of the leading edge synthetic jet. The reason is that the flow control mechanism at high frequency region is fundamentally different from that at low frequency region, which will be explained in the next part.

3.2.3 Flow control mechanism in terms of jet frequency

Based on the analyses of the previous flow control results, it was observed that the flow control mechanism could be characterized by the non-dimensional frequency of the synthetic jet. The characteristics of the flow control mechanism could be divided into two types according to the variation of the non-dimensional frequency: a low frequency jet (F1) and a high frequency jet (F5).

When the non-dimensional frequency was low (F1 or F2), a small vortex was formed due to a long period of synthetic jet motion, viscous force and jet inclined angle. Figure 6(a) shows the snapshots of local flow structure at four different phases: start of blowing (0°), maximum blowing (90°), start of suction (180°) and maximum suction (270°). As shown in the figures, the controlled case had a small vortex shedding periodically from the synthetic jet slot. The small vortex moved along the suction surface and penetrated to the large leading edge separation vortex flow, and as a result, the size of the leading edge separation vortex substantially decreased. This was somewhat contrasted with the uncontrolled case, at which the whole suction region was dominated by a large reverse flow (Fig. 4). As explained schematically in Fig. 7(a), the momentum supplied by the synthetic jet was exhausted for the generation of the small vortex.

Figure 6(b) shows the typical flow feature in case of high jet frequency (F5). In this case, the small vortex did not grow enough to penetrate into the large separation vortex because the period of synthetic jet motion was too short. Therefore, the synthetic jet could not perturb the separated flow with a smaller vortex and the lift enhancement was not noticeable compared to low frequency case. However, the flow near the synthetic jet slot was firmly attached, and as a result, more stable flow was induced on the suction surface. Figure 7(b) explains its aerodynamic consequence schematically. As shown in Fig. 7(b), the 'virtual' geometry of the airfoil in the controlled case (F5) is formed by the combined shape of the main airfoil with the separated flow. And the freestream

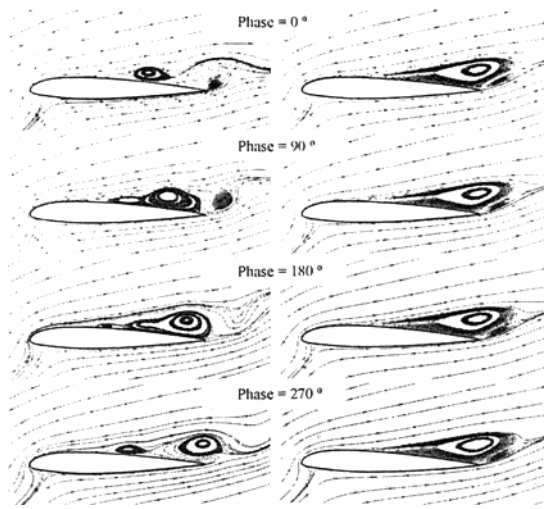

(a) F1V3 (b) F5V3

Fig. 6. Phase-locked streamlines (AOA 22°).

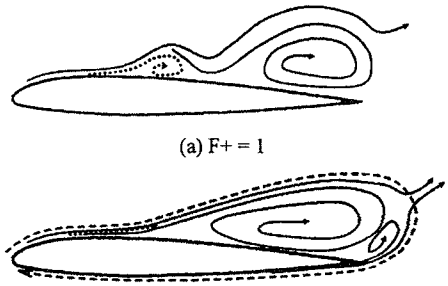

(a) F+ = 1

(b) F+ = 5

Fig. 7. Schematic of circulation change (AOA 22°).

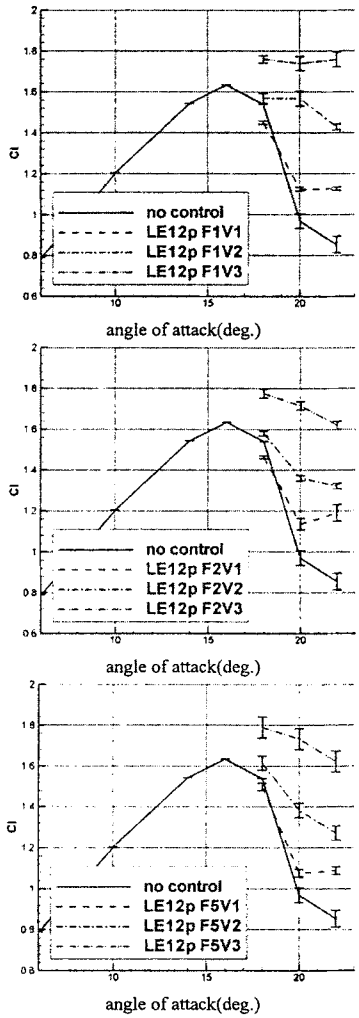

Fig. 8. Lift coefficient on NACA23012 with a 12% chord synthetic jet.

flowed around the virtual airfoil shape formed by both the airfoil and the separated flow on the suction surface. Thus a portion of the supplied momentum

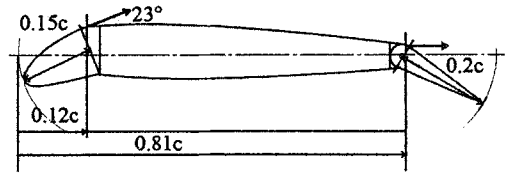

Fig. 9. Geometry of NACA23012 with leading edge droop and plain flap.

from the synthetic jet contributed to the temporal change of airfoil circulation, as shown Fig. 7(b). In other words, the circulation around the virtual airfoil was enhanced or reduced depending on the phase of the high frequency synthetic jet. At the blowing phase, circulation was enhanced while circulation was reduced at the suction phase. Thus the temporal fluctuation of the lift coefficient was larger than those at low frequency range (Fig. 8).

3.2.4 Combination of synthetic jet and simple high lift device

Based on the previous results, most effective conditions of separation control using a synthetic jet could be summarized as follows. The non-dimensional frequency of the synthetic jet is 1, at which the lift coefficient increased much more than other frequencies. The lift coefficient increases with synthetic jet momentum at the same non-dimensional frequency. And, when the synthetic jet is located at the separation point, maximal lift can be obtained.

Those effective conditions were applied to an airfoil with a simple high lift device. The non-dimensional frequency was fixed to 1, and the separation point was fixed by introducing the leading droop and plain flap, at which the synthetic jet was located. This is described in Fig. 9. A NACA23012 with a 15% chord leading edge droop and 20% plain flap was simulated. The leading edge droop was deflected 20°, and the plain flap was deflected 30°. The inclined angle of the synthetic jet was 23° and the synthetic jet velocity was the triple of the freestream velocity. In this case, the characteristic length was the distance between the positions of the synthetic jet and the trailing edge, which are used for the calculation of the non-dimensional frequency.

As shown in Fig. 10 the combination of the synthetic jet with the simple high lift device produced the similar aerodynamic performance as the conventional fowler flap system. In Fig. 11, the flow patterns around the simple high lift device with and without

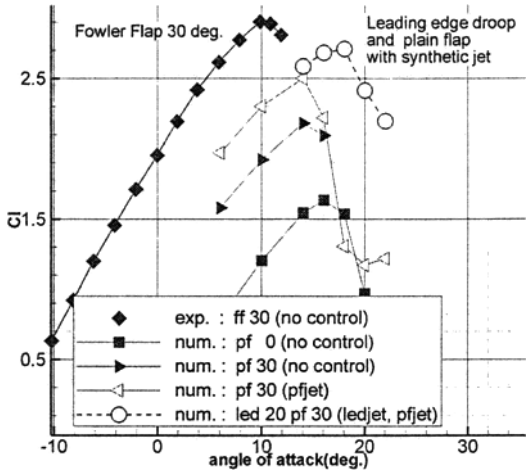

Fig. 10. Lift coefficient curves (ff: fowler flap, pf: plain flap, led: leading edge droop).

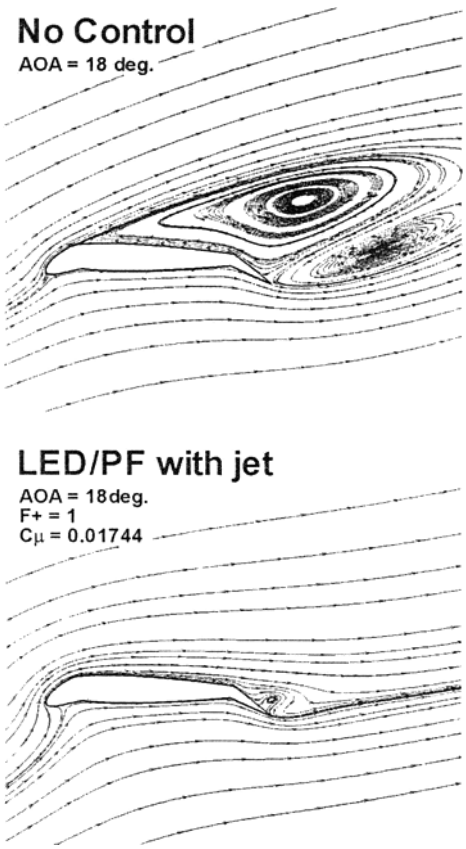

Fig. 11. Phase-averaged streamlines.

the synthetic jet are compared. These results confirmed that aerodynamic characteristics were remarkably improved by the leading edge droop with the synthetic jet near the separation point and by the plain flap with the synthetic jet at the flap leading edge.

4. Summary

In this work, we presented the numerical simulation results of flow control using a synthetic jet on a NACA23012 airfoil with a 20% plain flap at Reynolds number of 2.19×10^6 for various angles of attack, jet velocities and jet frequencies. Moreover, we confirmed that the synthetic jet was able to move the separation point and thus change the global flowfield structure efficiently. Consequently, stall characteristics and control surface performance were remarkably improved by using a synthetic jet.

The aerodynamic characteristics of the flow control could be divided into two types according to the variation of the non-dimensional frequency. For low frequency, a small vortex penetrated to the large separated flow at the leading edge, which led to the substantial size reduction of the leading edge separation vortex. For high frequency, on the other hand, the small vortex did not grow enough to penetrate into the large separation vortex. Instead, the synthetic jet firmly attached the local flow and changed the circulation of the virtual airfoil shape. The maximum lift was obtained when the separation point coincided with the synthetic jet location and the non-dimensional frequency was 1. In addition, separation control was effective as the peak velocity of the synthetic jet increased.

Although a small vortex generated by the synthetic jet greatly affected the separation control and lift force enhancement, it might possess a side effect that induced local flow structure to be easily broken by external disturbance or gust. Beside, if the required peak velocity is too large, the weight and size of the synthetic jet also would increase, which may hamper the efficient design and manufacture of a flow control system based on synthetic jet. Therefore, further research to reduce the amplitude of the synthetic jet peak velocity without compromising separation control capability is necessary.

Acknowledgements

Authors are gratefully acknowledging the financial supports by Agency for Defense Development and FVRC (Flight Vehicle Research Center, Seoul National University), the Brain Korea 21 Project in 2006 and the Smart UAV Development Program of

the 21th Frontier R&D Program sponsored by the Ministry of Commerce, Industry and Energy.

Nomenclature

c : Chord length
h : Slot width
U_∞ : Freestream velocity
f : Frequency of periodic excitation
C_μ : Momentum coefficient, $(A_{jet}/U_\infty)^2 h/c$
$F+$: Non-dimensional frequency, fc/U_∞

References

Abbott, I. H. and Doenhoff, A. E., 1959, "Theory of Wing Sections," Dover Publications Inc.

Amitay, M., Smith, D., Kibens, V., Parekh, D. and Glezer, A., 2001, "Aerodynamic Flow Control over an Unconventional Airfoil using Synthetic Jet Ac-tuators," *AIAA Journal*, Vol. 39, No. 3, pp. 361~370.

Bardina, J. E., Huang, P. G. and Coakley, T. J., 1997, "Turbulence Modelling Validation, Testing and Development," NASA TM-110446.

Chatlynee, E., Rumigny, N., Amitay, M. and Glezer, A., 2001, "Virtual Aero-shaping of a Clark-Y Airfoil using Synthetic Jet Actuators," *AIAA paper 2001-0732.*

Chorin, A. J., 1968, "Numerical Solution of the Navier-Stokes Equations," *Mathematics of Computation*, Vol. 22, pp. 745~762

Collins, F. G. and Zelenevits, J., 1975, "Influence of Sound upon Separated Flow over Wing," *AIAA Journal*, Vol. 13, No. 3, pp. 408~410.

Donovan, J. K., Kral, L. D. and Cary, A. W., 1998, "Active Flow Control Applied to an Airfoil," *AIAA paper 98-0210.*

Gad-el-Hak, M., 2002, "The MEMS handbook," CRC press, Boca Raton, Florida.

Ho, C. M. and Tai, Y. C., 1998, "Micro-Electro-Mechanical System (MEMS) and Fluid Flow," *Annual Review of Fluid Mechanics*, Vol. 30, pp. 579~ 612.

Kim, C. S., Kim, C. and Rho, O. H., 2000, "Parallel Computations of High-lift Airfoil Flows using Two-equation Turbulence Models," *AIAA Journal*, Vol. 38, No. 8, pp. 1360~1368.

Kral, L. D., Donovan, J. F., Cain, A. B. and Cary, A. W., 1997, "Numerical Simulation of Synthetic Jet Actuators," *AIAA paper 97-1824.*

Nagib, H. et al., 2003, DARPA XV-15 TiltRotor Micro Adaptive Flow Control (MAFC) flight presentation, URL: http://fdrc.iit.edu/research/nagibResearch.php

Ravi, B. R., Mittal, R. and Najjar, F. M., 2004, "Study of Three-dimensional Synthetic Jet Flowfields using Direct Numerical Simulation," *AIAA paper 2004-0091.*

Seifert, A. and Pack, L. G., 1999, "Oscillatory Control of Separation at High Reynolds Numbers," *AIAA Journal*, Vol. 37, No. 9, pp. 1062~1071.

Seifert, A., Bachar, T., Wygnanski, I., Koss, D. and Shepshelovich, M., 1993, "Oscillatory Blowing, a Tool to Delay Boundary Layer Separation," *AIAA Journal*, Vol. 31, No. 11, pp. 2052~2060.

Smith, B. L. and Glezer, A., 2002, "Jet Vectoring using Synthetic Jets," *Journal of Fluid Mechanics*, Vol. 458, pp. 1~34.

Wenzinger, C. J. and Harris, T. A., 1939, "Wind-tunnel Investigation of an NACA23012 Airfoil with Various Arrangements of Slotted Flaps," NACA Re-port No. 664.

Yoon, S. and Kwak, D., 1991, "Three-dimensional Incompressible Navier-Stokes Solver Using Lower-Upper Symmetric Gauss-Seidel Algorithm," *AIAA Journal*, Vol. 29, No. 6, pp. 874~875.